Non-Adaptive Robust Filters for Speckle Noise Reduction

ALEJANDRO C. FRERY[1]
SIDNEI J. S. SANT'ANNA[2]

Instituto Nacional de Pesquisas Espaciais
Divisão de Processamento de Imagens
(INPE - DPI)
Avenida dos Astronautas, 1758
12227-010 São José dos Campos, SP
Brazil
[1]frery@dpi.inpe.br
[2]sidnei@dpi.inpe.br

Abstract. After briefly reviewing some classical filters for speckle removal, five filters with characteristics of robustness, suitable for speckle noise reduction, are derived and implemented. These filters are the ones based on the trimmed maximum likelihood and moments estimators, the ones based on the median, on the inter-quartile range and on the median absolute deviation. Assuming that observations within a synthetic aperture radar image are outcomes of independent Rayleigh random variables, these filters exhibit a good performance from both the signal-to-noise reduction and from the edge preserving criteria. The problem of filtering in an image is posed as an estimation problem.

Key Words: estimation, filtering, maximum likelihood, multiplicative models, order statistics, robustness, speckle, statistics, synthetic aperture radar.

1 Introduction

Image processing techniques have suffered an explosive growth in the last years. This is due to, among other reasons, the fact that more and more information from different sources, in the form of images, is available. It is known that about 50% of the images sent by environmental satellites has never been seen by human eyes... and that most of them carry precious information.

That information, when retrieved within an acceptable delay after its acquisition, is present in our daily life: from relevant information about the weather, to statistics about continental growth of crops that take part in decisions about international financial aids, including information for ships about drifting icebergs.

Therefore, it is becoming of crucial importance the ability to process images rapidly, and in such a manner that the relevant information within these images is accurately retrieved. Within this context, statistical ideas are becoming very important. Other tools, such as the ones derived fron Artificial Intelligence, are also contributing to the development of techniques for the processing and the interpretation of images.

Synthetic Aperture Radar (SAR) images are receiving an increasing attention, mainly due to the several satellites already launched, not to mention the airborne missions. This kind of imaging, besides providing dielectrical and textural information of the targets, is little affected by adverse atmospheric conditions, such as fog, rain, clouds, etc. It also allows night imaging, since the sensor is active and carries its own illumination source.

The main problem with the use of SAR images is a kind of signal-dependent noise: *speckle* noise. It makes difficult the visual and the automatic interpretation of the data, since it produces a salt-and-pepper effect.

Some classical algorithms for speckle reduction are reviewed: the mean, Frost, σ-Lee, Lee and the Kuan/Nathan filters.

In this work some filters for the reduction of speckle noise are derived. They have robust properties (in a sense to be defined): a desired characteristic for filtering algorithms. These filters are derived through the use of a statistical modelling of the data, and considering the ocurrence of edges and sharp features: the kind of feature that is desirable to retain after the filtering.

Their robustness is achieved through admitting that they might be applied to samples of contami-

nated observations. Then, five filters are proposed: two based upon the trimming of extreme observations, and three based upon order statistics.

These filters are easy to implement and they are not adaptive yielding, thus, an affordable computational effort.

2 Speckle Noise Filters

Several techniques for filtering whilst preserving relevant features in images have appeared in the literature (see [Nagao–Matsuyama (1979)], for example).

Some specialized filters have been proposed aiming at the reduction of speckle noise and, simultaneously, not blurring the image. The reader is referred to the papers [Frost et al. (1982)], [Lee (1981a, 1981b)], [Nathan–Kurlander (1987)], and to the references therein for details. Some of them are summarized in the following list:

- Mean filter: it consists of a local smoothing of the observations. It also normalizes the filtered image, but introduces severe blurring.
- Frost filter: it is a linear convolutional proposal, derived from the minimization of the mean quadratic error over a multiplicativel noise model. Dependence among observations is incorporated through an exponential spatial correlation function. It is adaptative.
- σ-Lee Filter: it assumes a normal distribution, and trimmes those observations beyond the $2\widehat{\sigma}$ interval.
- Lee Filter: a multiplicative noise model is adopted. It is a local linear minimum mean square error filter, since it uses a linearization, by Taylor expansion, around the mean. This approximation transforms the multiplicative model into an additive one, and then the Wiener filter is applied.
- Kuan/Nathan Filter: it is similar to the previous one. The difference is that this filter does not make any approximation. It is, also, an adaptative proposal.

3 Notation and Important Distributions

A model-based approach is adopted in order to design filters with good statistical properties. It is necessary, then, to introduce the following formalism.

Random variables will be denoted with uppercase letters, and their outcomes with lowercase ones, i.e.: X denotes a random variable, and x denotes an outcome of X. Random vectors will be denoted in boldface type; for the previous case, and its corresponding outcome, $\mathbf{X}$ and $\mathbf{x}$ would have been written, respectively.

The indicator function of the set A will be denoted $\mathbb{1}_A(x)$, i.e.:

$$\mathbb{1}_A(x) = \begin{cases} 1 & \text{if } x \in A \\ 0 & \text{if not.} \end{cases}$$

The cardinality of A is denoted $\#A$. The set of the integers will be denoted $\mathbf{Z}$, the set of the real numbers $\mathbb{R}$, the set of the positive real numbers will be written $\mathbb{R}^+$, and the set of natural numbers $\mathbb{N} = \{1, 2, \ldots\}$.

A random variable with standard normal distribution will be denoted Z_i, i.e., its density is

$$f_{Z_i}(z) = \frac{1}{\sqrt{2\pi}} \exp\left(-\frac{1}{2}z^2\right) \text{ for every } z \in \mathbb{R}.$$

A random variable W has a χ distribution with $\tau > 0$ degrees of freedom, and this ditribution will be denoted χ_τ, if its density is

$$f_W(w) = \frac{w^{\tau-1}}{2^{\frac{\tau}{2}}\Gamma\left(\frac{\tau}{2}\right)} \exp\left(-\frac{w^2}{2}\right) \mathbb{1}_{\mathbb{R}^+}(w).$$

The k-th moment of W is given by

$$\mathbb{E}(W^k) = 2^{\frac{k}{2}} \frac{\Gamma\left(\frac{\tau+k}{2}\right)}{\Gamma\left(\frac{\tau}{2}\right)}, \tag{1}$$

where the Euler's Gamma function is given by

$$\Gamma(\nu+1) = \int_{\mathbb{R}^+} t^\nu \exp(-t)\, dt, \text{ for every } \nu > -1,$$

and holds that $\Gamma(k) = (k-1)!$ if $k \in \mathbb{N}$. Other useful properties of this function can be seen in [Graham et al., 1988].

It is possible to see in [Koroliuk, 1986] that the distribution of a random variable V defined, for every $n \in \mathbb{N}$, by

$$V = \sqrt{\sum_{1 \le i \le n} Z_i^2}$$

is χ_n if, for every $i \neq j$, Z_i is independent of Z_j. Statisticians often use the distribution of the random variable V^2, called χ^2 distribution with n degrees of freedom, and denoted χ^2_n.

We shall be interested in the χ_2 distribution, called standard Rayleigh distribution. It is the distribution of the distance of a point in $\mathbb{R}^2$ to the origin that, starting from $(0,0)$, *walks* in each axis a random and independent standard normal quantity.

Let $\xi \in \mathbb{R}^+$, it is said that Y is a Rayleigh random variable with parameter ξ (and this random variable will be denoted $Y \sim \mathcal{R}(\xi)$) if its density is

$$f_\xi(y) = \frac{y}{\xi^2} \exp\left(-\frac{1}{2}\left(\frac{y}{\xi}\right)^2\right) \mathbb{1}_{\mathbb{R}^+}(y). \tag{2}$$

Its cummulative distribution function is obtained integrating with respect to y:

$$F_\xi(t) = \left[1 - \exp\left(-\frac{1}{2}\left(\frac{t}{\xi}\right)^2\right)\right] \mathbb{1}_{\mathbb{R}^+}(t); \quad (3)$$

this function shall be neccessary for the calculation of the filters.

The reader can easily check that if $X \sim \mathcal{R}(1)$, then $\xi X \sim \mathcal{R}(\xi)$, i.e., Rayleigh random variables form a scale family of distributions.

Let $F\colon \mathbb{R} \longrightarrow [0,1]$ be the cummulative distribution function of an arbitrary random variable Y, and $0 < \alpha < 1$, then the α-quantile of Y is defined as $\inf\{t \in \mathbb{R}\colon F(t) \geq \alpha\}$. This quantity will be denoted y_α.

Using equation (3) it is immediate to obtain the α-quantile of a $\mathcal{R}(\xi)$ distributed random variable:

$$y_\alpha = \xi\sqrt{2\ln\frac{1}{1-\alpha}},$$

and, therefore, its median and inter-quartile range are, respectively,

$$\begin{aligned} \mathrm{Med}(Y) &= y_{\frac{1}{2}} = \xi\sqrt{2\ln 2}, \text{ and} && (4)\\ \mathrm{IQR}(Y) &= y_{\frac{3}{4}} - y_{\frac{1}{4}} = \\ &\qquad \xi\left(\sqrt{2\ln 4} - \sqrt{2\ln\frac{4}{3}}\right). && (5) \end{aligned}$$

If $Y \sim \mathcal{R}(\xi)$, then its expected value and variance are given, using equation (1) and the scale property, by

$$\mathbb{E}(Y) = \sqrt{\frac{\pi}{2}}\,\xi \text{ and } \mathrm{Var}(Y) = \left(2 - \frac{\pi}{2}\right)\xi^2, \quad (6)$$

respectively. The density of Y, equation (2), is shown in Figure 1 for two different values of the parameter ξ. The value of the parameters for these densities was obtained applying the maximum likelihood estimator (equation (13)) over homogeneous areas of the image shown in Figure 2.

Some other important properties of this distribution are

$$\begin{aligned} \mathbb{E}\left(Y - \mathbb{E}(Y)\right)^k &= \left(\sqrt{2}\xi\right)^k \frac{k}{2}\Gamma\left(\frac{k}{2}\right) && (7)\\ \gamma_1 &= \frac{2\sqrt{\pi}(\pi-3)}{(4-\pi)^{3/2}} && (8)\\ \gamma_2 &= \frac{32-3\pi^2}{(4-\pi)^2} && (9)\\ m(Y) &= \xi, && (10) \end{aligned}$$

where equations (7), (8), (9) and (10) are, respectively, the kth moment about zero, the skewness, the kurtosis and the mode of $Y \sim \mathcal{R}(\xi)$. Notice that the quantities (8) and (9) do not depend on the parameter ξ.

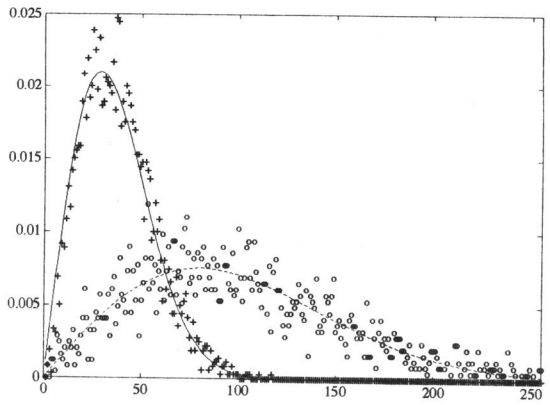

Figure 1: Histograms ("+" and "o" resp.) and estimated Rayleigh densities (continuous and dashed lines, resp.) for the dark and light regions: $\xi = 28.90$ and $\xi = 77.90$ respectively.

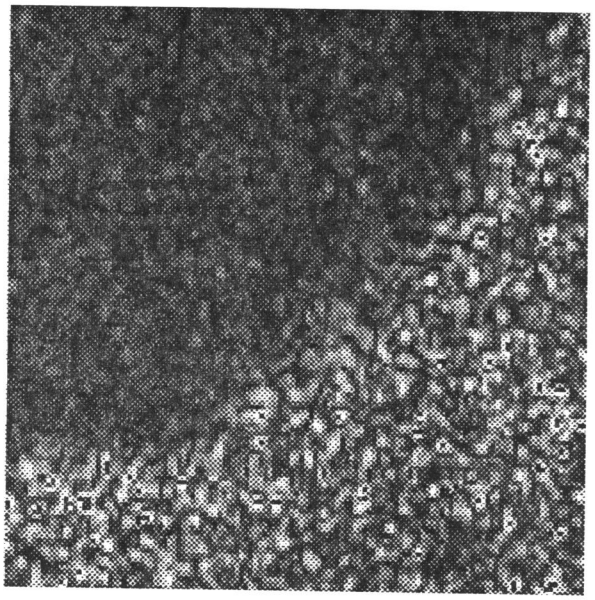

Figure 2: Image SAR-580, L band.

For every $x \in \mathbb{R}^+$ its integer part will be denoted as $\lfloor x \rfloor$, i.e., $\lfloor x \rfloor = \max\{k \in \mathbb{N}\colon k \leq x\}$. For notational ease, the set of even numbers is denoted $\mathcal{E}$, and the set of odd numbers $\mathcal{O}$.

Let now $\mathbf{a} = (a_1, \ldots, a_n)$ be a n-dimensional vector of real numbers, and $\mathbf{a}_A$ a subset of $\mathbf{a}$, where $\mathbf{a}_A = \{a_j\}$ with $j \in A \subset \{1, \ldots, n\}$. The vector $\mathbf{a}$ sorted in ascending order will be denoted $\mathbf{a}_{(\bullet)}$, where $\mathbf{a}_{(\bullet)} = (a_{n:1}, \ldots, a_{n:n})$ (i.e. $a_{n:1} \leq a_{n:2} \leq \cdots \leq a_{n:n}$). The sample median of $\mathbf{a}$ is denoted as

$$Q_2(\mathbf{a}) = \begin{cases} a_{n:\lfloor n/2 \rfloor + 1} & \text{if } n \in \mathcal{O} \\ \frac{1}{2}(a_{n:n/2} + a_{n:n/2+1}) & \text{if } n \in \mathcal{E}; \end{cases}$$

the lower sample quartile of **a** as

$$Q_1(\mathbf{a}) = \begin{cases} a_{n:(\ell+1)/2} & \text{if } \ell \in \mathcal{O} \\ \frac{1}{2}(a_{n:\ell/2} + a_{n:\ell/2+1}) & \text{if } \ell \in \mathcal{E}; \end{cases} \quad (11)$$

and the upper sample quartile of **a** as

$$Q_3(\mathbf{a}) = \begin{cases} a_{n:(n+1-(\ell+1)/2)} & \text{if } \ell \in \mathcal{O} \\ \frac{1}{2}(a_{n:n+1-\ell/2} + a_{n:n-\ell/2}) & \text{if } \ell \in \mathcal{E}. \end{cases} \quad (12)$$

In equations (11) and (12) it was written:

$$\ell = \begin{cases} \frac{n-1}{2} & \text{if } n \in \mathcal{O} \\ \\ \frac{n}{2} & \text{if } n \in \mathcal{E}. \end{cases}$$

4 Properties of SAR Images

The support of the image will be denoted S. It is defined as a finite subset of $\mathbf{Z}^2$ of the form $S = S_1 \times S_2$, with $S_i = \{a_i, \ldots, b_i\} \subset \mathbf{Z}$ for $i = 1, 2$.

Within the SAR image processing community, the parameter ξ of the Rayleigh distributions is called "backscatter". One of the most accepted hypothesis is that the marginal distribution of observations obeys a Rayleigh law, due to the presence of speckle noise.

Assuming that the *ground truth* is a collection of positions, each with one among L possible values $0 < \xi_1 < \cdots < \xi_L < +\infty$ of backscatter, the imaging system returns, for that position, the outcome of a Rayleigh random variable with the corresponding parameter. This is the *multiplicative model* proposed for this kind of imaging.

This degradation model, that changes an unobserved ground truth into an observed image, is a particular case of the model studied in [Bustos–Frery (1992)]. This is equivallent to supposing that, given the terrain backscatter, the speckle noise is independent from pixel to pixel and that the imaging was obtained with one look and linear detection. Three complete references for these subjects are the papers [Goodman (1982)], [Kelly et al. (1988)], [Derin et al. (1990)], and the references therein.

This hypothesis could be verified, for example, using the χ^2 and/or the Kolmogorov-Smirnov tests. Another simple way of doing it is estimating $C(Y)$, the variation coefficient within homogeneous regions and checking that it is approximately constant since from equations (6), holds that

$$C(Y) = \frac{\sigma(Y)}{\mathrm{I\!E}(Y)} = 2\sqrt{\frac{1}{\pi} - \frac{1}{4}}.$$

Assuming valid this hypothesis, and since the true value of the parameter of the distribution is not known, this parameter could be estimated using a vector of observations $\mathbf{y} = (y_1, \ldots, y_v)$ by means of, for instance, the maximum likelihood estimator

$$\widehat{\xi}_{\mathrm{ML}} = \sqrt{\frac{1}{2v} \sum_{1 \le i \le v} y_i^2}. \quad (13)$$

This estimator possesses all the desirable properties of asymptotic efficiency and consistency.

Another estimator that frequently appears in the literature is the one based upon the first sample moment, given by the following equation:

$$\widehat{\xi}_{\mathrm{MO}} = \frac{1}{v}\sqrt{\frac{2}{\pi}} \sum_{1 \le i \le v} y_i. \quad (14)$$

Notice that the previous estimator, multiplied by the factor $\sqrt{\pi/2}$, yields the sample mean of the observations.

In this work, the problem of filtering an image shall be posed as the problem of estimating parameters within a window of that image. Therefore, in principle, the estimators given by equations (13) or (14) could be used.

These estimators have a good behaviour when the observations within the considered sample are the outcomes of collectivelly independent identically distributed Rayleigh random variables. This could not be the case in real images due to several reasons, the most evident is when the filter is acting over or close to edges between regions with different backscatters or sharp features; other reason is correlation among the observations, a phenomenum that may appear depending on the imaging system.

When at least one of the hypothesis above is not valid, it is said that the sample comes from a *contaminated* model; else, the model is said to be *pure*. These models are carefully defined in the following section.

5 The Models

As it was said before, two situations are considered: one (Definition 5.1) is when the filter is applied to homogeneous observations; the other (Definition 5.2), when observations from different populations are being filtered. Independence among random variables is always assumed. Let v be a positive integer and $\xi > 0$.

Definition 5.1 *The random variables $Y_1, \ldots, Y_v$ satisfy a pure Rayleigh model with parameter ξ if they are independent identically distributed random variables each with density f_ξ.*

Definition 5.2 *The random variables $Y_1, \ldots, Y_v$ satisfy a contaminated Rayleigh model with parameter ξ and lower contamination proportion α (with $\alpha > 0$); scale of lower contamination ξ_0 (with $0 < \xi_0 < \xi$); upper contamination proportion β (with $\beta > 0$ and $\alpha + \beta < \frac{1}{2}$), and scale of upper contamination ξ_2 (with $\xi < \xi_2 < +\infty$) if: $Y_1, \ldots, Y_v$ are independent; $Y_1, \ldots, Y_{\lfloor \alpha v \rfloor}$ are identically distributed, each with density f_{ξ_0}; $Y_{\lfloor \alpha v \rfloor + 1}, \ldots, Y_{v - \lfloor \beta v \rfloor}$ are identically distributed, each with density f_ξ; and $Y_{v - \lfloor \beta v \rfloor + 1}, \ldots, Y_v$ are identically distributed, each with density f_{ξ_2}.*

A situation where this *contaminated* model is applied could be, for example: $v = 9$, $\xi_0 = 10$, $\xi = 50$, $\xi_2 = 90$, $\alpha = 0$ and $\beta = 0.3$. In this case, nine observations of independent random variables are to be used in order to estimate the parameter ξ; six of them are outcomes of a f_ξ-distributed random variable, the other three are outcomes of a f_{ξ_2}-distributed random variable, with $\xi < \xi_2$.

6 Robust Filters

[Bovik et al. (1983)], [Kie-Bum–Kashyap (1987)] and [Kundu et al. (1984)] are some references to the use of robust techniques in image processing. Two quite complete texts for a general approach to robustness in statistical inference are [Barnett–Lewis, 1978] and [Bustos, 1981], among others.

In this work two kinds of robust estimators will be considered: two based upon the idea of *trimming* extremal observations, and three based on *order statistics* [Frery–Sant'Anna (1993)].

Proceeding with the idea that *filtering* is *estimating*, and taking into account the possibility of having a contaminated sample of observations, the use of the following estimators is proposed (they are all based upon the sample $\mathbf{y}_W$, of size v):

$$\widehat{\xi}_{\mathrm{TML}} = \sqrt{\frac{1}{2(v-2a)} \sum_{i=a+1}^{v-a} y_{v:i}^2} \qquad (15)$$

$$\widehat{\xi}_{\mathrm{TMO}} = \sqrt{\frac{2}{\pi}} \frac{1}{v-2a} \sum_{i=a+1}^{v-a} y_{v:i} \qquad (16)$$

$$\widehat{\xi}_{\mathrm{MAD}} = \frac{1}{K_1} Q_2(\mathbf{z}_W), \qquad (17)$$

$$\widehat{\xi}_{\mathrm{IQR}} = \frac{Q_3(\mathbf{y}_W) - Q_1(\mathbf{y}_W)}{K_2}, \qquad (18)$$

$$\widehat{\xi}_{\mathrm{Med}} = \frac{1}{K_3} Q_2(\mathbf{y}_W), \qquad (19)$$

where $a = \lfloor v\alpha_0 \rfloor$, $0 \leq \alpha_0 < 1/2$, and $(y_{v:1}, \ldots, y_{v:v})$ denotes the vector $\mathbf{y}_W = (y_1, \ldots, y_v)$ sorted in ascending order; $\mathbf{z} = (z_1, \ldots, z_v)$, with $z_i = |y_i - Q_2(\mathbf{y})|$ for every $i \in W$. The trimmed observations are the $\lfloor v\alpha_0 \rfloor$ smallest and the $\lfloor v\alpha_0 \rfloor$ biggest ones.

The equations above are: the *trimmed ML* estimator with a proportion of deleted observations equal to $2\alpha_0$ (equation (15)), the *trimmed MO* estimator with a proportion of deleted observations equal to $2\alpha_0$ (equation (16)), the MAD (*Median Absolute Deviation*) estimator (17), the IQR estimator based on the inter-quartile range (18), and the Median estimator (19).

The constants K_1, K_2 e K_3 are calculated, in order to make the respective estimators asymptotically consistent, in the following manner: for K_2 and K_3 it is enough to know $y_{1/4}$, $y_{1/2}$ and $y_{3/4}$, and to apply the substitution method. In this way, using equations (4) and (5), the values $K_2 = \sqrt{2 \ln 4} - \sqrt{2 \ln 4/3}$ and $K_3 = \sqrt{2 \ln 2}$ are obtained.

The constant K_1 can be obtained using numerical tools, and its approximate value is $K \approx 0.4485$. In order to obtain this value, it is neccessary to know the distribution of the random variable $Z = |X - \mathrm{Med}(X)|$, where $X \sim \mathcal{R}(1)$, and to define $K_1^{-1} = \mathrm{Med}(Z)$.

In order to retain the mean grey level of the image, the estimated values must be related to the expected value of the Rayleigh distribution. This is achieved using equation (6) and, thus, multiplying the estimated parameters by the factor $\sqrt{\pi/2}$.

The following situation will be always considered: only those pixels with a *proper* number of neighbours shall be filtered; those not satisfying this property will remain unfiltered. The original and filtered images will be denoted $\mathbf{y} = [y_s]_{s \in S}$ and $\widehat{\mathbf{x}} = [\widehat{x}_s]_{s \in S}$, respectively. Any of the filters above will be denoted $\mathcal{F}$; it is a function of the form $\mathcal{F}: \Xi^W \longrightarrow \Xi$, where Ξ is the range for every pixel (for instance, $\Xi = \{0, \ldots, 255\}$ was used in our implementations).

The support of the filter was written W. It is a "square" of size $2t+1$ centered on the origin: $W = \{-t, \ldots, 0, \ldots, t\} \times \{-t, \ldots, 0, \ldots, t\}$. So, the filter involves $v = (2t+1)^2$ observations for every filtered pixel. Let us also define the translation of W by the point $r = (r_1, r_2)$ as $W_r = \{s \in \mathbf{Z}^2 : s - r \in W\}$.

Finally, the operation of applying a filter to an image can be written, for every $s \in S$, as

$$\widehat{x}_s = \begin{cases} \sqrt{\frac{\pi}{2}} \mathcal{F}(\mathbf{y}_{W_s}) & \text{if } W_s \subset S \\ y_s & \text{if not.} \end{cases} \qquad (20)$$

If there would be the need to filter every pixel in the image, the definition (20) could be modified, in order to fit the different cases of $\#(W_s \cap S)$. It was preferred not to do so in order to simplify the computations and, by the way, to use the unfiltered observations of the image as a fast form of checking the

overall noise reduction. Other shapes for W could also be used as, for example, the ones derived from the notion of a *L-norm*: $W = \{s \in S: \|s\|_L \leq d\}$, where $s = (s_1, s_2)$, $d \in \mathbb{N}$ and

$$\|s\|_L = \begin{cases} |s_1| + |s_2| & \text{if } L = 1, \\ \sqrt{s_1^2 + s_2^2} & \text{if } L = 2 \text{ and} \\ \max\{|s_1|, |s_2|\} & \text{if } L = \infty. \end{cases}$$

A slight modification ought to be introduced in the definitions of all the estimators above, in order to have the same range, Ξ (a discrete finite set) for the original and filtered images. The closest integer to the filtered value is used, i.e., $\lfloor \frac{1}{2} + \sqrt{\frac{\pi}{2}} \mathcal{F}(\mathbf{y}_{W_s}) \rfloor$.

Moreover, if all the observations within the window W had the same value, then the IQR and MAD estimators would be zero; they are then redefined as $\widehat{\xi}_{\text{IQR}}(\mathbf{y}_W) = \widehat{\xi}_{\text{MAD}}(\mathbf{y}_W) = Q_1(\mathbf{y}_W)$ if $y_{v:1} = y_{v:v}$.

It is then clear that, whatever the filter used, $\widehat{\mathbf{x}} = [\widehat{x}_s]_{s \in S}$ is an estimator of the unobserved image $\mathbf{x} = \sqrt{\pi/2}\,[\xi_s]_{s \in S}$ based on the observed image $\mathbf{y} = [y_s]_{s \in S}$ justifying, thus, the notation.

7 Results

The presented techniques are applied to an airborne SAR (L band) image obtained over the region of Freiburg, Germany.

Figure 2 is a 128×128 pixels part of the original image, where speckle noise is evident. Also, it has two distinguishable regions: the darker one, bare soil; and forest, the lighter one.

Figures 3, 4, 5, 6, 7, 8, 9 are, respectively, the images filtered by the ML, MO, TML, TMO, MAD, IQR and Med algorithms. All the images were generated with the use of a filter of size $t = 5$, and the trimming algorithms used a value $\alpha_0 = 0.225$.

In order to assess the noise reduction $\widehat{C^{-1}}$, the reciprocal of the coefficient of variation (signal-to-noise relation) within homogeneous regions was used. The estimated values of skewness and kurtosis relate the relative "normality" of observations.

Table 1 shows the values, rounded to the third decimal place, for a total number of 3500 observations taken from to the darker region.

Table 2 shows the values, rounded to the third decimal place, for a total number of 2679 observations taken from to the lighter region.

The observed values of both coefficient of variation and skewness, in both subareas, is "close enough" to the theoretical value, therefore, not revealing evidence against the use of Raighley distributions.

The best algorithm with respect to the $\widehat{C^{-1}}$ criterion is the maximum likelihood (ML) estimator: it yieds an increase of about 107% and of about 139%

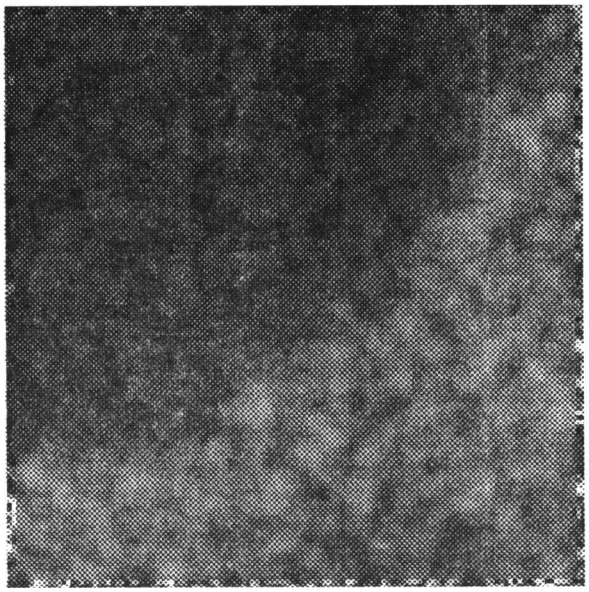

Figure 3: ML filtered image.

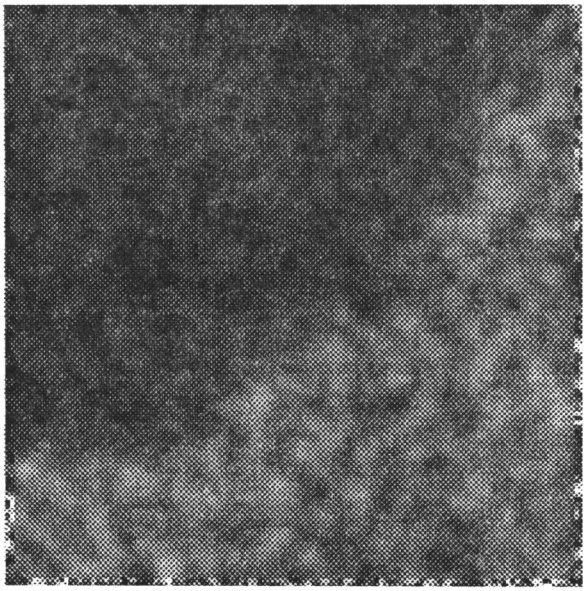

Figure 4: MO filtered image.

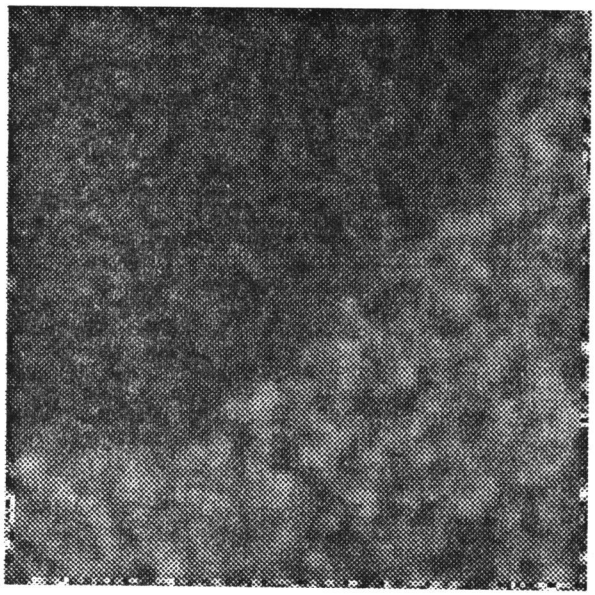

Figure 5: TML filtered image.

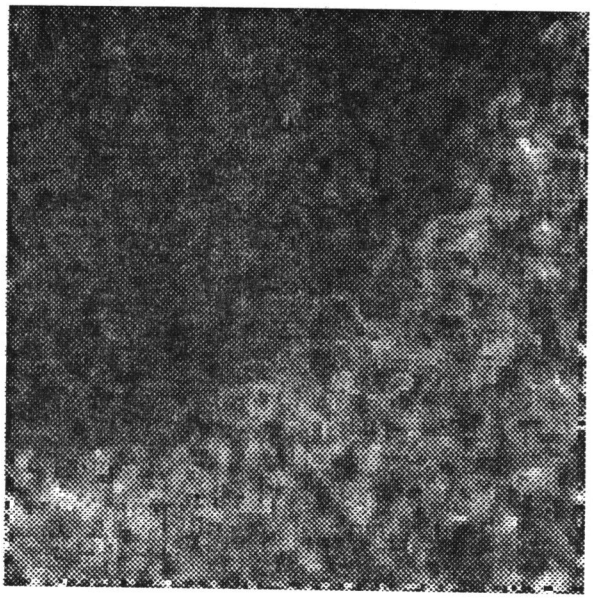

Figure 7: MAD filtered image.

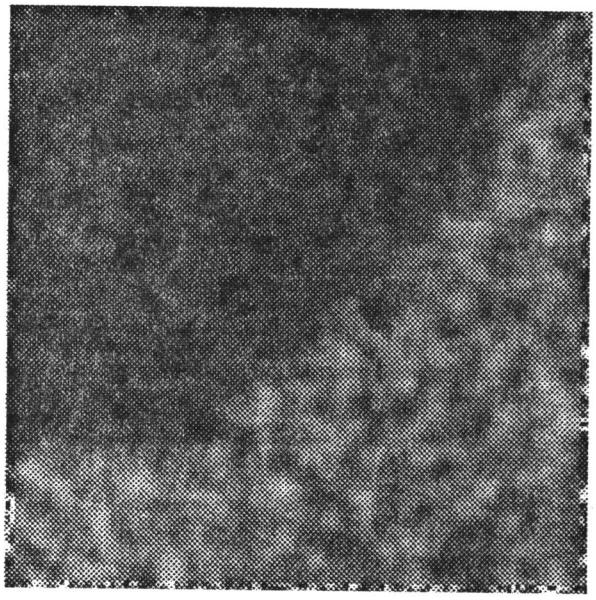

Figure 6: TMO filtered image.

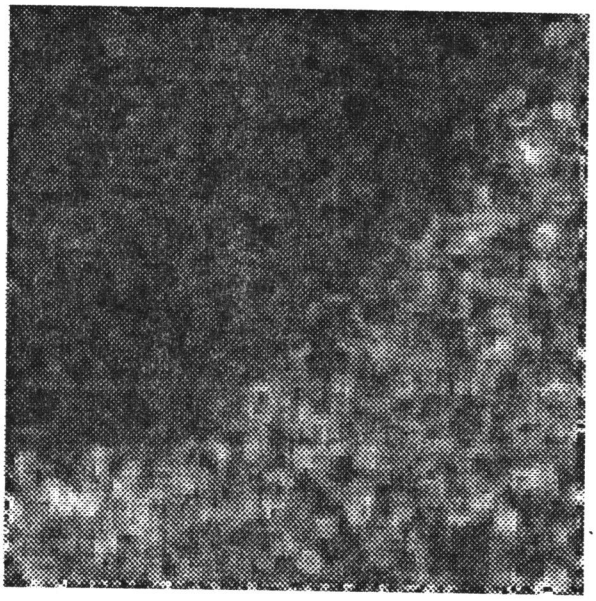

Figure 8: IQR filtered image.

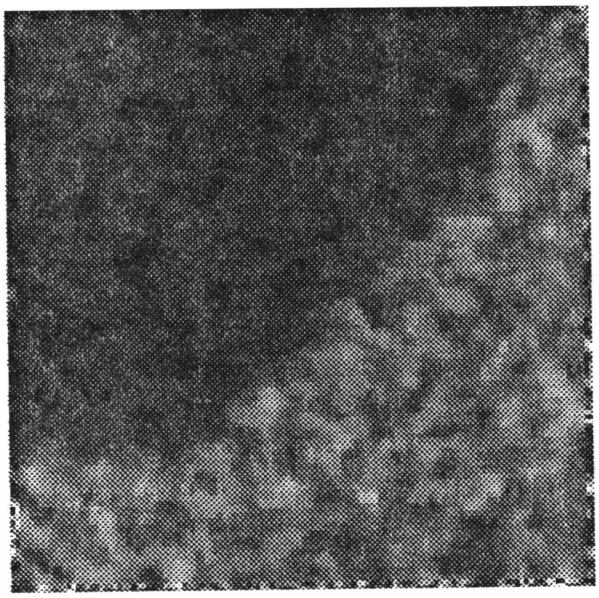

Figure 9: Med filtered image.

	$\widehat{C^{-1}}$	Skewness	Kurtosis
Theoretical	1.913	0.631	3.245
Original	1.965	0.665	0.276
ML	4.060	1.593	8.366
MO	4.057	1.419	7.061
TML	3.881	1.688	8.206
TMO	4.018	1.201	5.296
MAD	3.088	0.914	2.061
IQR	3.082	1.103	2.364
Med	3.881	0.960	3.429

Table 1: Estimated values over the dark area

	$\widehat{C^{-1}}$	Skewness	Kurtosis
Theoretical	1.913	0.631	3.245
Original	1.879	0.573	−0.155
ML	4.494	0.683	4.100
MO	4.424	0.660	3.472
TML	4.140	0.903	3.820
TMO	4.199	0.595	2.135
MAD	3.155	0.627	0.652
IQR	3.185	0.611	0.579
Med	3.971	0.491	1.100

Table 2: Estimated values over the light area

	Dark Area	Light Area
ML	107%	139%
MO	106%	135%
TML	98%	120%
TMO	105%	124%
MAD	57%	68%
IQR	57%	70%
Med	98%	111%

Table 3: Noise reduction over homogeneous areas

for the dark and ligh areas, respectively. The *worst* robust algorithm with respect to the same criterion is the MAD (about 57% and 68%, for the same areas); see Table 3. Thus, the difference is not too strong, whilst the induced blurring is less severe with the worst of these techniques than with the use of the ML equation. The edge preserving property of the filters proposed can be checked making a visual comparison between them and the ML filter.

It is imporant to keep in mind that, in general, it is not possible to say that a certain filter is *the best*. The choice of a particular filter deppends on the application.

Figure 10 shows the histograms of the original and filtered images. It is evident that, after filtering, there is a separation of classes. Before filters are applied the histogram of the whole image is unimodal inducing, thus, to a confusion between classes.

8 Additional Information and Extensions

The algorithms were implemented, in a single program, in the C++ programming language; the SUN's C++ compiler, V. 2 was used. The results shown in this work were obtained running the program in a SUN SPARCstation 2, under OpenWindows V. 3 and UNIX V. 4.1.1. The required time to obtain all the filtered images was 9 seconds, for the considered window (the bigger the window, the slower the execution: notice that two sortings —both carried out with calls to an internal "quicksort" function provided with the programming language— are applied over vectors of size $v = (2t + 1)^2$ for every filtered pixel).

Displays and hardcopies were obtained with the SAO (Smithsonian Astrophysical Observatory) image utility, and estimations with the KHOROS system. The constant K_1 and Figures 1 and 10 were obtained using the tools provided with the Pro-Matlab V. 3.5h system.

The performace of new constants $K_1(v)$, $K_2(v)$

and $K_3(v)$ that make (17), (18) and (19) *unbiased* estimators under the pure model, is being evaluated against the already defined ones. Also, proper scaling values for the same purpose are being tested for equations (15) and (16).

The authors intend to continue this work by proposing other robust filters and by using Monte Carlo techniques for the assessment of the relative quality of these techniques. This quality shall be measured in terms of consistency, efficiency and edge preservation. Different proportions of contamination and of their parameters values will be considered, along with the determination of suitable values of the constant α_0.

Quantitative techniques, rather than the *qualitative* evaluation here proposed, for the assessment of the (undesired) blurring induced by the filters are under evaluation.

Listings are available, through e-mail, upon request.

9 Acknowledgement

The authors are grateful to Professors O. H. Bustos (Facultad de Matemática, Astronomía y Física, Universidad Nacional de Córdoba, Argentina) and N. D. A. Mascarenhas (Instituto Nacional de Pesquisas Espaciais, Brazil) for their continous help and stimulus.

10 References

Barnett, V.; Lewis, T. *Outliers in statistical data.* Great Britain, John Wiley & Sons, 1978.

Bovik, A.C.; Huang, T.S.; Munson, D.C. A generalization of median filtering using linear combination of order statistics. *IEEE Trans. on Acoustics, Speech and Signal Processing*, ASSP-31:1342–1349, 1983.

Bustos, O.H. *Estimação robusta no modelo de posição.* Poços de Caldas, XIII Colóqio Brasileiro de Matemática, 1981.

Bustos, O.H.; Frery, A.C. A contribution to the study of Markovian degradated images: an extension of a theorem by Geman and Geman. *Matemática Aplicada e Computacional*, 11:17–29, 1992.

Derin, H.; Kelly, P.; Vézina, G.; Labbit, S. Modelling and segmentation of speckled images using complex data. *IEEE Trans. on Geoscience and Remote Sensing*, GRS-28:76–87, 1990.

Frery, A.C.; Sant'Anna, S.J.S. Redução de ruído em imagens SAR pelo uso de filtros robustos. Simpósio Brasileiro de Sensoriamento Remoto, 7., Curitiba, maio 1993. *Anais.* São José dos Campos, INPE/SBC, 1993. To appear.

Frost, V.S.; Stiles, J.A.; Shanmugan, K.S.; Holtzman, J.C. A model for radar images and its applications to adaptive digital filtering of multiplicative noise. *IEEE Trans. on Pattern Analysis Machine Intelligence*, PAMI-4:157–166, 1982.

Goodman, J.W. Statistical properties of laser speckle patterns. In: Dainty, J.C., ed. *Laser Speckle and Related Phenomena*, chap. 2, Springer-Verlag, 1982.

Graham, R.; Knuth, D.; Patashnik, O. *Concrete mathematics: a foundation for computer science.* USA, Addison-Wesley, 1988.

Kelly, P.; Derin, H.; Hartt, K. Adaptive segmentation of speckled images using a hierarchical random field model. *IEEE Trans. on Acoustics, Speech and Signal Processing*, ASSP-36:1628–1641, 1988.

Kie-Bum, E.; Kashyap, R.L. Robust image model based noise supression. In: *The Scandinavian Conference on Image Analysis*, 5., Stockholm, June 2–5, 1987.

Koroliuk, V. *Manual de la teoría de probabilidades y estadística matemática.* 1. rep. Moscú, Editorial Mir, 1986.

Kundu, A.; Mitra, S.K.; Vaidyanathan, P.P. Application of two-dimensional generalized mean filtering for removal of impulse noises from images. *IEEE Trans. on Acoustics, Speech and Signal Processing*, ASSP-32:600–609, 1984.

Lee, J.S. Speckle analysis and smoothing of synthetic aperture radar images. *Computer Graphics and Image Processing*, 17:24–32, 1981a.

Lee, J.S. A simple speckle smoothing algorithm for synthetic aperture radar images. *IEEE Trans. on Systems, Man, and Cybernetics*, SMC-13:85–89, 1981b.

Nagao, M.; Matsuyama, T. Edge preserving smoothing. *Computer Graphics and Image Processing*, 9:394–407, 1979.

Nathan, K.S.; Kurlander, J.C. Speckle noise reduction of 1-look SAR imagery. In: *Procedings of IGARSS'87 Symposium.* Ann Harbour, 18–21 May 1987.

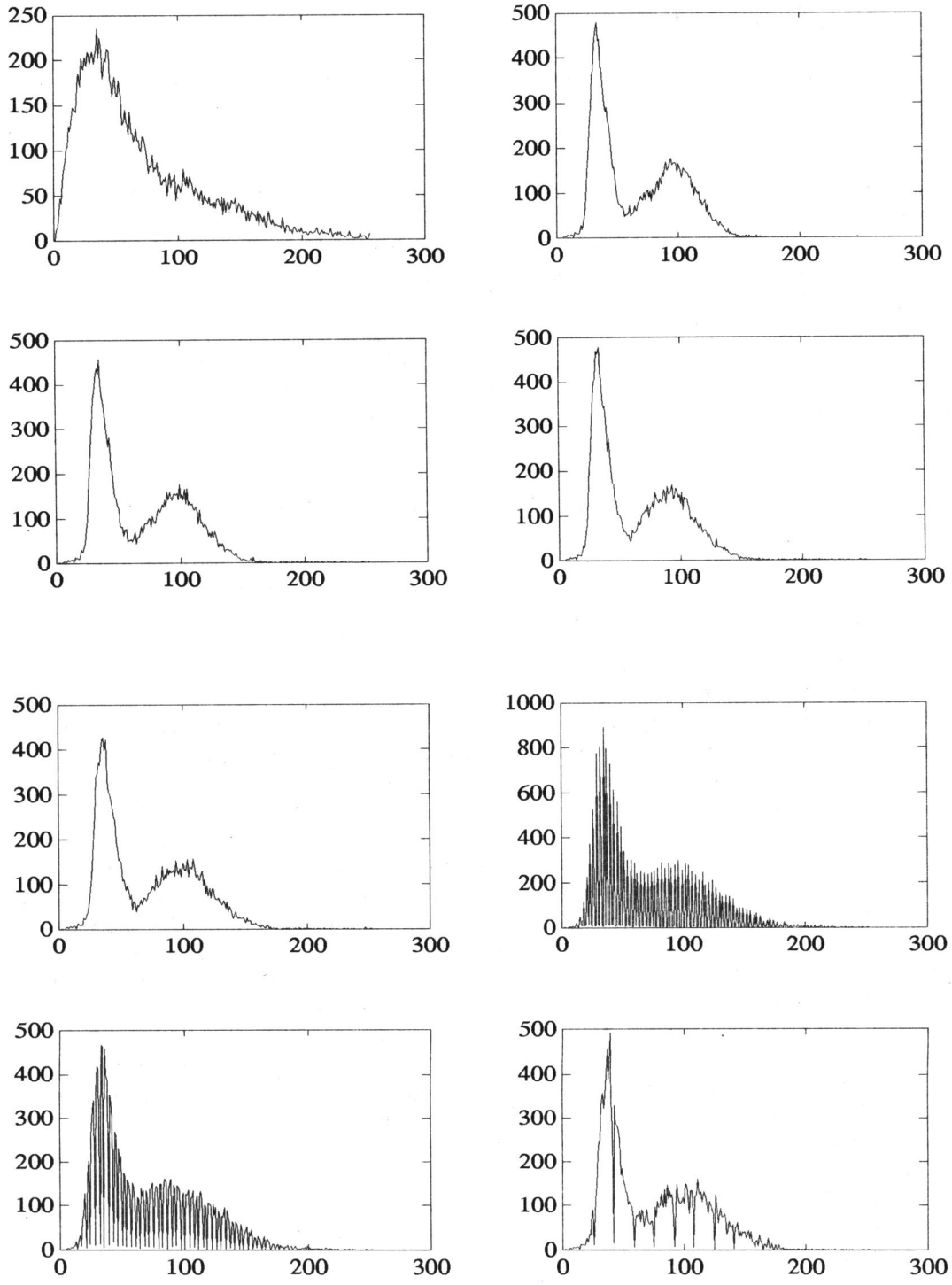

Figure 10: Histograms, left to right and up to down, of the original image and of the ML, MO, TML, TMO, MAD, IQR and Med filtered images.